

# Universality of photon counting below a bifurcation threshold

Lisa Arndt\* and Fabian Hassler

*JARA Institute for Quantum Information, RWTH Aachen University, 52056 Aachen, Germany*

(Dated: September 2020)

At a bifurcation point, a small change of a parameter causes a qualitative change in the system. Quantum fluctuations wash out this abrupt transition and enable the emission of quantized energy, which we term photons, below the classical bifurcation threshold. Close to the bifurcation point, the resulting photon counting statistics is determined by the instability. We propose a generic method to derive a characteristic function of photon counting close to a bifurcation threshold that only depends on the dynamics and the type of bifurcation, based on the universality of the Martin-Siggia-Rose action. We provide explicit expressions for the cusp catastrophe without conservation laws. Moreover, we propose an experimental setup using driven Josephson junctions that exhibits both a fold and a pitchfork bifurcation behavior close to a cusp catastrophe.

Universality is a central theme in modern statistical mechanics. A prime example is the universality of the critical exponents that describe the divergence of observables close to a second-order phase transition [1–3]. Catastrophe theory offers insights into the universality as it categorizes how small changes in external parameters can lead to qualitative changes in the behavior of the system [4]. As such, it also provides a suitable framework to study phase transitions in driven-dissipative systems [5–8]. In these system, finite frequency excitations are studied—which we call photons in the following. At the bifurcation threshold, a small change of the system parameters leads to a condensation of these photons [9]. Typical examples are the lasing [10] and the Dicke transition [11] in optical systems.

In the vicinity of a bifurcation point, a characteristic long time-scale emerges in the dissipative dynamics of the system. As a result, the qualitative properties of phase transitions can be described only by a small number of relevant degrees of freedom exhibiting the slow dynamics. Moreover, a (quasi-)classical treatment of the dynamics is appropriate since the number of photons becomes large in the vicinity of the bifurcation threshold. Note that the dynamics of slow classical degrees of freedoms has been grouped into universality classes by Halperin and Hohenberg [12].

Different types of bifurcations and dynamics in driven-dissipative systems lead to a variety of critical exponents and correlation behaviors that have been the focus of many studies in recent years [13–24]. So far, mirroring the discussion of equilibrium physics, these exponents are derived for low-order cumulants of physical observables. Note that in equilibrium physics, the central limit theorem leads to a Gaussian statistics of all relevant observables and moreover the fluctuations are connected to the amount of dissipation. On the other hand, in driven-dissipative systems the fluctuation-dissipation theorem does not hold and even more importantly non-Gaussian statistics should be expected in general which leads to the question of determining the critical exponents of higher order cumulants.

Motivated by this insight, we employ a path integral formalism [25–30] to investigate the photon counting statistics below the bifurcation threshold. We find that the critical exponents of all the cumulants only depend on the type of bifurcation given a Halperin-Hohenberg dynamics. In particular, this result explains that the full counting statistics of the degenerate [29, 31] and non-degenerate parametric oscillator [32, 33] are equivalent close to the threshold, as was noted in Ref. [33]. Based on the universality of the Martin-Siggia-Rose action, we propose a generic method to derive a universal characteristic function of photon counting close to a bifurcation threshold. We exemplify our formalism for a cusp catastrophe with a system dynamics without conservation laws. We note that the universality of counting statistics in non-equilibrium systems has been discussed before in different contexts, *e.g.*, for the statistics of topological defects [34, 35], particle transport [36, 37], and non-equilibrium fluctuation theorem [38, 39].

The article is organized as follows. Our starting point is the classical description of the bifurcation dynamics by the corresponding Martin-Siggia-Rose action. From there, we derive a universal expression for the characteristic function of photon counting below the bifurcation threshold by including a normal-ordered counting term. To demonstrate the formalism, we analyze the counting statistics and rare event statistics for a fold and a pitchfork bifurcation within a cusp catastrophe framework. Finally, we propose a microwave experiment that can demonstrate the critical exponents in the higher order cumulants of the cusp catastrophe.

Each model in the Halperin-Hohenberg classification can be mapped to a corresponding classical Martin-Siggia-Rose action  $S_{MSR}$ . In the following, we want to consider photon radiation with a linewidth  $\Gamma$  and frequency  $\Omega \gg \Gamma$  that emanates from a system close to a driven-dissipative phase transition. For simplicity, we focus on a single harmonic oscillator whose ‘slow’ dynamics in the rotating frame is purely dissipative. In the Halperin-Hohenberg classification, this dynamics corresponds to universality class A also known as the Glauber

model. Our results apply mutatis mutandis to dissipative field theories which are relevant to lattices of coupled cavities, see *e.g.* Refs. [20, 40, 41].

For our system, the Martin-Siggia-Rose action of the dimensionless ‘slow’ variable  $x$  is given by  $S_{\text{MSR}}(x, \tilde{x}, \beta) = \int dt \tilde{x} [\dot{x} + \Gamma x - f(x) + \frac{i}{2}\beta\Gamma\tilde{x}]$  with the response field  $\tilde{x}$  which satisfies the commutation relation  $[x, \tilde{x}] = i$ . This action corresponds to a Langevin equation of the form  $\dot{x} = -\Gamma x + f(x) + \xi(t)$ . The Gaussian fluctuations  $\xi(t)$  have the correlations  $\langle \xi(t) \rangle = 0$  and  $\langle \xi(0)\xi(t) \rangle = \beta\Gamma\delta(t)$ , with a classical, temperature-dependent noise parameter  $\beta \propto k_B T / \hbar\Omega$ . The term  $-\Gamma x$  corresponds to the dissipative part of the force in the rotating frame. The remaining force  $f(x) = -V'(x)$  is non-dissipative and includes the external driving force.

In the quantum description of the system, a parameter  $\alpha$  is introduced that relates the quadrature  $x^2$  to the photon number  $n = x^2/\alpha$ . In this sense,  $\alpha$  plays the role of  $\hbar$ . We are interested in the quasi-classical regime with  $\alpha \ll 1$  where the quantum fluctuations remain small [42, 43]. We relate the variable  $\tilde{x}$  to the quantum scale by introducing the conjugate variable  $p = \alpha\tilde{x}$  with the canonical commutation relation  $[x, p] = i\alpha$ . Additionally, as we are interested in the quantum regime with  $k_B T \ll \hbar\Omega$ , where fluctuations are dominated by quantum effects, we have to replace  $\beta$  by  $\alpha$  [44]. The characteristic function of the photon counting statistics can be obtained by adding a source term to the Martin-Siggia-Rose action such that the generating function of the photon counting statistics is given by  $\mathcal{Z}(\chi) = \int \mathcal{D}[x]\mathcal{D}[p] \exp[iS(\chi)]$  with

$$S(\chi) = S_{\text{MSR}}(x, \alpha^{-1}p, \alpha) + \frac{\chi\Gamma}{\alpha} \int_0^\tau dt (x + \frac{i}{2}\alpha p)^2, \quad (1)$$

where  $\tau$  is the detection time. The generating function  $\mathcal{Z}(\chi)$  represents the characteristic function of the number of photons  $N$  detected within the time  $\tau$ ; from this, all the cumulants can be obtained via  $\langle\langle N^k \rangle\rangle = d^k \ln(\mathcal{Z}) / d(i\chi)^k |_{\chi=0}$ .

The special form of the last term in Eq. (1) is one of the main results of our work. It originates from the normal-ordering of the photon number operator  $\hat{n} = \hat{x}^2/\alpha$  and is a pure quantum effect. It can be understood as follows: using the conventional creation and annihilation operators  $\hat{b}^\dagger$  and  $\hat{b}$ , the normal-ordered operator is of the form  $:\hat{x} := (\alpha/2)^{1/2}(\hat{b}_-^\dagger + \hat{b}_+)$ , with the notation  $\hat{O}_+(\rho) = \hat{O}\rho$  and  $\hat{O}_-(\rho) = \rho\hat{O}$  where  $\rho$  is the density operator. An equivalent way of writing the normal-ordered operator is given by  $:\hat{x} := \hat{x}_s + \frac{i}{2}\alpha\hat{p}_a$ , with  $\hat{x}_s = \frac{1}{2}(\hat{x}_+ + \hat{x}_-)$ ,  $\hat{p}_a = \hat{p}_+ - \hat{p}_-$ , and  $\hat{p} = i(\alpha/2)^{1/2}(\hat{b}^\dagger - \hat{b})$ . Since the operators  $\hat{x}_s$  and  $\hat{p}_a$  are canonically conjugate with  $[\hat{x}_s, \hat{p}_a] = i\alpha$ , they correspond to the variables  $x$  and  $p$  in the quasi-classical action. Note that the normal ordering leads to the additional terms  $i\alpha xp - \frac{1}{4}\alpha^2 p^2$  when expanding  $(x + \frac{i}{2}\alpha p)^2$  that are coupled to the counting field but vanish in the classical limit  $\alpha \rightarrow 0$  (at fixed  $x, \tilde{x}$ ).

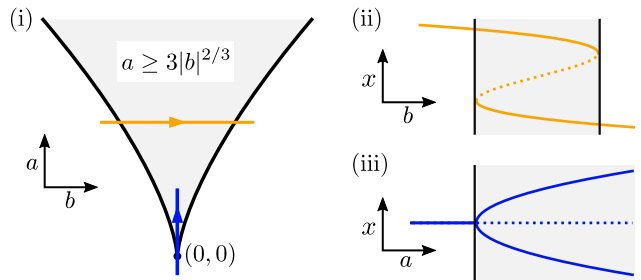


FIG. 1. (i) Cusp shape in the canonical variables  $(a, b)$ . The fold bifurcation lines at  $b = \pm(a/3)^{3/2}$  separate the region outside the cusp, where a single stable solution exists, from the region inside the cusp (gray) where two stable solutions exist. (ii) Evolution of the fixed points as the systems passes through the cusp along the horizontal line indicated in (i). At the first fold bifurcation, a second stable solution (solid line) and an unstable point (dotted line) become available, while the stability of the upper point remains unchanged. The classical switch between both solutions takes place at the second fold bifurcation, where the upper fixed point and the unstable fixed point merge forcing the system onto the lower, stable fixed point. (iii) Evolution of the fixed points as the systems passes to  $a > 0$  through the cusp point  $(0, 0)$  along the vertical line indicated in (i). At the pitchfork bifurcation, the single stable fixed point splits into two stable (solid lines) and one unstable (dotted line) solution.

In the first part of this paper, we have shown how the characteristic function close to bifurcation can be obtained purely from the knowledge of the classical Martin-Siggia-Rose action. In the following, we exemplify this method by calculating the counting statistics for the explicit choice of the potential  $V(x)/\Gamma = x^4 - ax^2/2 + bx$ , with the dimensionless parameters  $a$  and  $b$  [45]. This potential corresponds to a cusp catastrophe which enables us to study the two most fundamental bifurcations: the fold and the pitchfork bifurcation. In the following, we elaborate on and demonstrate the introduced method by calculating explicitly the critical exponents and rare-event statistics for both types of bifurcations.

In the parameter space  $(a, b)$ , the system can be divided into two regions: the first region, outside the cusp, where a single stable solution exists and the second region, inside the cusp, where two stable solutions exist. The cusp shape is shown in Fig. 1(i). It is formed by the lines  $b = \pm(a/3)^{3/2}$  for  $a \geq 0$ .

In the symmetrical case  $b = 0$ , the system displays a pitchfork bifurcation as it passes to  $a > 0$  through the cusp point  $(0, 0)$ . Here, one stable, classical solution splits into two stable solutions and one unstable solution as displayed in Fig. 1(iii). Away from the cusp point, the system displays a fold bifurcation, where in addition to the single stable solution that already exists outside the cusp an alternate second solution that is paired with an unstable solution becomes available. Disregarding fluctuations, the classical state of the system does not change

upon this transition due to hysteresis. Instead, the classical switch between both solutions takes place at the second fold bifurcation as indicated in Fig. 1(ii). Here, the initial classical solution vanishes forcing the system onto the second fixed point.

First, we want to calculate the counting statistics in the vicinity of the pitchfork bifurcation at  $(0, 0)$ , with  $\delta = -a > 0$  the distance from the bifurcation point. For  $b = 0$ , this corresponds to the counting statistic of the parametric oscillator which has already been analyzed in Refs. [29, 33]. In the quasi-classical limit  $\alpha \ll 1$ , vacuum phase fluctuations remain small. Upon approaching the threshold, the fluctuations increase. However, for sufficiently small  $\alpha$ , the crossover region where the fluctuations become of the order of 1 remains narrow and can be estimated as  $\delta \simeq \alpha$ . It is therefore valid to expand the Martin-Siggia-Rose action to quadratic order around the stationary solution below the instability threshold. For  $|b| \ll \delta$ , the stationary solution is given by  $x = p = 0$ .

We focus on the limit of long measurement times  $\Gamma\tau \gg 1$  and calculate the cumulant-generating function  $\lambda(z = i\chi) = \ln[\mathcal{Z}(\chi)]$ . In the vicinity of the threshold, we obtain the result

$$\lambda(z) = \frac{\Gamma\tau}{2} \left[ \delta - \sqrt{\delta^2 - 2z} + \frac{2b^2z}{\alpha(\delta^2 - 2z)} \right] \quad (2)$$

which corresponds to the cumulants

$$\frac{\langle\langle N^k \rangle\rangle}{\Gamma\tau} = \frac{(2k-3)!!}{2\delta^{2k-1}} + \frac{2^{k-1}k!b^2}{\alpha\delta^{2k}}. \quad (3)$$

The counting statistics has two distinct contributions: The first term is due to the pure pitchfork statistics at  $b = 0$  which has been previously reported in Refs. [29, 33]. The second term is due to the contribution of the fold at finite  $b$ . Note that the cumulants diverge as  $\delta^{-\gamma_k}$  with  $\gamma_k$  the critical exponent of the  $k$ -th cumulant. The pitchfork yields  $\gamma_k = 2k-1$  which, for  $k = 1$ , reproduces the critical exponent of the number of photons in the cavity in a Dicke model discussed in Ref. [11]. The fold contribution demonstrates an even stronger divergence with  $\gamma_k = 2k$ . At finite but small  $b$ , we thus predict a crossover behavior with the critical exponent changing from  $2k-1$  to  $2k$  when approaching the threshold [1]. The Fano factor  $F = \langle\langle N^2 \rangle\rangle / \langle N \rangle$  is a measure of the number of correlated photons. For the pure pitchfork statistic this factor is given by  $F = \delta^{-2} \propto n^2$  with  $n = \langle N \rangle / 2\Gamma\tau$  the average number of photons in the system. Thus, the number of correlated photons exceeds by far the number of photons present in the system at any given time [29]. The photons are thus correlated over the long, divergent time scale  $\tau^* = F/\bar{I} = 2/\Gamma\delta$ , with  $\bar{I} = \langle N \rangle / \tau$  the average photon current. This is a central characteristic of the bifurcation behavior. The divergent time scale is also responsible for the large deviations from the average photon current. In particular, the probability to measure a photon current

$I$  during the measurement time  $\tau$  is given by

$$P(I) \propto \exp \left[ -\frac{\tau}{2\tau^*} \left( \frac{\bar{I}}{I} + \frac{I}{\bar{I}} - 2 \right) \right], \quad (4)$$

up to exponential accuracy [29, 33]. Note that the probability distribution is strongly asymmetric with the probability to measure a current smaller than average currents strongly suppressed when compared to the Gaussian approximation.

Next, we want to compare the results of the pitchfork to the fold bifurcation which is the instability away from the cusp point. In this regime, two saddle points contribute to the counting statistics which correspond to the two stable solutions above the transition. Note that the second saddle point is at a finite value of the quantum variable  $p$  since there is only a single stable classical solution below the transition. Analogously to the calculation at the cusp point, we want to avoid the crossover region close to the bifurcation point where phase fluctuations increase without bounds. For the fold bifurcation, this narrow region can be estimated as  $\delta \simeq \alpha^2 b^{-4/3}$ , where we introduced the measure  $\delta = 3b^{2/3}(3b^{2/3} - a) > 0$  for the distance to the bifurcation [46]. Away from this region, both saddle points are well separated and the total cumulant-generating function is given by  $\lambda(z) = \ln[p_1 e^{\lambda_1(z)} + p_2 e^{\lambda_2(z)}]$ , with  $\lambda_{1,2}(z)$  the cumulant-generating function of the first/second saddle point. The probabilities  $p_j$ , with  $p_1 + p_2 = 1$ , denote the fraction of time the  $j$ -saddle point contributes to the total counting statistics [25]. We find that the second saddle point is exponentially suppressed as compared to the first saddle point with  $p_2 \propto \exp(-\Gamma\tau\delta^{1/2})$ . This is due to the fact that the second saddle point is at a finite value of the quantum variable such that it is only probed by rare quantum fluctuations.

Evaluating  $\lambda_{1,2}$ , we find that only the second saddle point leads to a divergent counting statistics. Because of this, we require intermediate times,  $1 \ll \Gamma\tau \ll \delta^{-1/2}$ , to observe the critical exponents such that  $p_2 \approx p_1 \approx \frac{1}{2}$  and the relevant part of the counting statistics is given by  $\lambda(z) = \frac{1}{2}\lambda_2(z)$ . Note that at longer measurement times, the probability  $p_2$  to be at the second saddle point decreases exponentially reducing the prefactor of the divergences. At intermediate time scales, we obtain the result

$$\lambda(z) = \frac{\Gamma\tau b^{2/3} \delta z}{8\alpha(\delta - z)} \quad (5)$$

for the leading order behavior in  $\delta$  and  $b$  close to the bifurcation threshold with the cumulants

$$\frac{\langle\langle N^k \rangle\rangle}{\Gamma\tau} = \frac{k! b^{2/3}}{8\alpha \delta^{k-1}}. \quad (6)$$

In this case, the critical exponents  $\gamma_k = k-1$  are different from the pitchfork bifurcation. In particular, the

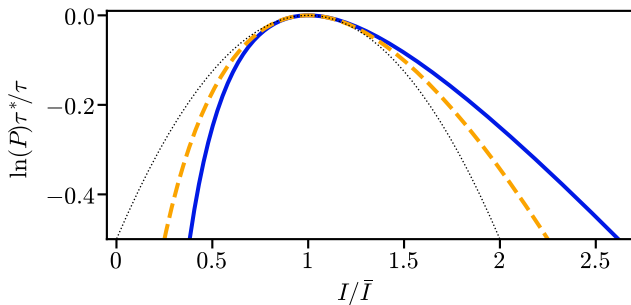


FIG. 2. Probability of large deviations of the photon current  $I$  from the average current  $\bar{I}$  in the vicinity of the pitchfork bifurcation (blue, solid line) and the fold bifurcation (orange, dashed line). The scaling is chosen such that both probabilities have identical Gaussian expansions around  $I = \bar{I}$  as indicated by the thin, dotted line. Note that both probabilities are strongly asymmetric leaning towards large current deviations.

photon current at the fold does not show any divergence and only the Fano factor  $F = 2\delta^{-1}$  shows a divergence. The diverging time-scale in this case is given by  $\Gamma\tau^* = 16ab^{-2/3}\delta^{-1}$  and only diverges as  $\delta^{-1}$  when compared to  $\delta^{-2}$  before. Note that the condition  $\delta \gtrsim \alpha^2 b^{-4/3}$  from above makes sure that we are in the intermediate regime with  $\Gamma\tau^* \lesssim \delta^{-1/2}$ . The rare-event statistics is given by

$$P(I) \propto \exp\left[-\frac{2\tau}{\bar{I}\tau^*}\left(I^{1/2} - \bar{I}^{1/2}\right)^2\right]. \quad (7)$$

In Fig. 2, we compare the probability of large deviation of both types of bifurcations. Compared to the Gaussian approximation, both types of bifurcation show an increased probability for larger photon currents. At fixed  $\bar{I}\tau^*$ , the pitchfork leads to larger fluctuations with  $|\ln P|_{\text{pitchfork}} \approx \frac{1}{4}|\ln P|_{\text{fold}}$ . For deviations below the average current, we observe that for the fold bifurcation the probability to observe a current  $I \rightarrow 0$  is finite  $P_{\text{fold}}(I \rightarrow 0) \propto \exp(-2\tau/\tau^*)$  whereas the corresponding probability vanishes in the pitchfork case.

Before concluding, we want to discuss possible experimental realizations in which the predicted exponents can be observed. The behavior of a Dicke transition [11] at finite number of spins can be mapped to a pitchfork bifurcation. Such a system is realized with cold-atomic gases in a cavity [8]. Measuring the statistics of the photons that are leaking out of the cavity will enable a comparison to the predicted critical exponents. The paradigmatic example of the fold bifurcation is the laser transitions (in rotating wave) [5, 6, 47] whose physical realizations are ubiquitous. We predict the counting statistics of the photons below the lasing transition to be universal and to follow Eq. (6). In the following, we highlight an implementation using superconducting circuits where the full cusp catastrophe, in particular the crossover from pitchfork to the fold transition, can be observed. The setup ex-

tends the circuit of Ref. [29] with an additional ac-current source to account for the asymmetry in the cusp potential. The total setup is composed of a Josephson junction with Josephson energy  $E_J$ , biased by a dc-voltage source, that is in series with a microwave resonator and an ac-current source. The resonator is characterized by a resonance frequency  $\Omega$ , the decay rate  $\Gamma$ , and an impedance  $Z_0$  at low frequency. To observe the cusp catastrophe, we set the frequency of the current source to the resonance frequency  $\Omega$  with  $I(t) = I_0 \sin(\Omega t)$  and tune the Josephson frequency  $\Omega$  with  $I(t) = I_0 \sin(\Omega t)$  and tune the resonance frequency to twice the resonance frequency by setting the dc-bias voltage to  $V = \hbar\Omega/e$ . Additionally, we require the phase between both drives to be fixed. We assume that the impedance far from resonance  $Z_0$  is small at the quantum scale such that the vacuum fluctuation strength  $\alpha = 8e^2 Z_0/\hbar \ll 1$  [48]. The calculation of the corresponding action follows similar steps as the derivations in Refs. [29, 33], *i.e.*, starting with a Keldysh path integral formalism and performing a rotating wave approximation. The final step is a projection of the resulting action onto the ‘slow’ direction of the dynamics in the vicinity of the cusp bifurcation line. It yields the Martin-Siggia-Rose action of the Glauber model for the force  $f(x)/\Gamma = 8\epsilon J_2(x)/x - j$  with the Bessel functions  $J_m(x)$  and the parameters  $j = \alpha I_0/4e\Gamma$  and  $\epsilon = \alpha E_J/4\hbar\Gamma$ . To discuss the behavior in the vicinity of the cusp catastrophe, it is sufficient to expand the Bessel function to fourth order in  $x$ . Then, the force is given by  $f(x)/\Gamma = -\epsilon x^3/12 + \epsilon x - j$ , which leads to a cusp bifurcation line at  $j = \pm \frac{4}{3}\epsilon^{-1/2}(\epsilon - 1)^{3/2}$  for  $\epsilon \gtrsim 1$ . For the counting statistic in the vicinity of the pitchfork bifurcation, the mapping to the previous parameters is straightforward with  $\delta = 1 - \epsilon$  and  $b = j$ . For the fold bifurcation, we obtain the mapping  $\delta = (\frac{3}{4}j)^{2/3}[(\frac{3}{4}j)^{2/3} - \epsilon + 1]$  and  $b = 48j$  to leading order in  $j$ .

In conclusion, we have outlined a method to derive the universal characteristic function of photon counting close to a bifurcation threshold. While our results focused on the Glauber model without any spatial dependence, our approach to derive the characteristic function from the classical Martin-Siggia-Rose action can be easily mapped to other models or problems with spatial dependence for which other universality classes can be studied. The most important step is the exchange of the classical counting term by its normal-ordered quantum equivalent. We have demonstrated the proposed method by calculating the photon counting statistics below the cusp threshold for the fold as well as the pitchfork bifurcation. Superficially, both bifurcations lead to a divergent counting statistics upon approaching the bifurcation threshold. However, the critical exponents  $\gamma_k$  as well as the probabilities of rare events differ. Possible ways to test the universal statistics include the lasing [47] and the Dicke transition [11]. Additionally, we have proposed a microwave setup based on the degenerate parametric oscillator [29] that

exhibits a cusp catastrophe and could thus be used to observe both sets of critical exponents in a single device.

---

\* lisa.arndt@rwth-aachen.de

- [1] P. M. Chaikin and T. C. Lubensky, *Principles of Condensed Matter Physics* (Cambridge University Press, 1995).
- [2] H. E. Stanley, Scaling, universality, and renormalization: Three pillars of modern critical phenomena, *Rev. Mod. Phys.* **71**, S358 (1999).
- [3] A. Pelissetto and E. Vicari, Critical phenomena and renormalization-group theory, *Physics Reports* **368** (6), 549 (2002).
- [4] R. Thomas and V. Arnol'd, *Catastrophe Theory* (Springer Berlin Heidelberg, 1986).
- [5] H. Haken, Cooperative phenomena in systems far from thermal equilibrium and in nonphysical systems, *Rev. Mod. Phys.* **47**, 67 (1975).
- [6] S. H. Strogatz, *Nonlinear Dynamics and Chaos: With Applications to Physics, Biology, Chemistry and Engineering* (Westview Press, 2000).
- [7] I. Carusotto and C. Ciuti, Quantum fluids of light, *Rev. Mod. Phys.* **85**, 299 (2013).
- [8] H. Ritsch, P. Domokos, F. Brennecke, and T. Esslinger, Cold atoms in cavity-generated dynamical optical potentials, *Rev. Mod. Phys.* **85**, 553 (2013).
- [9] M. A. Levin and X.-G. Wen, String-net condensation: A physical mechanism for topological phases, *Phys. Rev. B* **71**, 045110 (2005).
- [10] O. Svelto, *Principles of Lasers* (Springer US, 2010).
- [11] P. Kirton, M. M. Roses, J. Keeling, and E. G. Dalla Torre, Introduction to the dicke model: From equilibrium to nonequilibrium, and vice versa, *Advanced Quantum Technologies* **2** (1-2), 1800043 (2019).
- [12] P. C. Hohenberg and B. I. Halperin, Theory of dynamic critical phenomena, *Rev. Mod. Phys.* **49**, 435 (1977).
- [13] E. G. D. Torre, S. Diehl, M. D. Lukin, S. Sachdev, and P. Strack, Keldysh approach for nonequilibrium phase transitions in quantum optics: Beyond the dicke model in optical cavities, *Phys. Rev. A* **87**, 023831 (2013).
- [14] L. M. Sieberer, S. D. Huber, E. Altman, and S. Diehl, Dynamical critical phenomena in driven-dissipative systems, *Phys. Rev. Lett.* **110**, 195301 (2013).
- [15] F. Brennecke, R. Mottl, K. Baumann, R. Landig, T. Donner, and T. Esslinger, Real-time observation of fluctuations at the driven-dissipative dicke phase transition, *Proceedings of the National Academy of Sciences* **110** (29), 11763 (2013).
- [16] J. Raftery, D. Sadri, S. Schmidt, H. E. Türeci, and A. A. Houck, Observation of a dissipation-induced classical to quantum transition, *Phys. Rev. X* **4**, 031043 (2014).
- [17] G. Dagvadorj, J. M. Fellows, S. Matyjaśkiewicz, F. M. Marchetti, I. Carusotto, and M. H. Szymańska, Nonequilibrium phase transition in a two-dimensional driven open quantum system, *Phys. Rev. X* **5**, 041028 (2015).
- [18] D. Nagy and P. Domokos, Critical exponent of quantum phase transitions driven by colored noise, *Phys. Rev. A* **94**, 063862 (2016).
- [19] N. Šibalić, C. G. Wade, C. S. Adams, K. J. Weatherill, and T. Pohl, Driven-dissipative many-body systems with mixed power-law interactions: Bistabilities and temperature-driven nonequilibrium phase transitions, *Phys. Rev. A* **94**, 011401 (2016).
- [20] J. Marino and S. Diehl, Quantum dynamical field theory for nonequilibrium phase transitions in driven open systems, *Phys. Rev. B* **94**, 085150 (2016).
- [21] M. Biondi, G. Blatter, H. E. Türeci, and S. Schmidt, Nonequilibrium gas-liquid transition in the driven-dissipative photonic lattice, *Phys. Rev. A* **96**, 043809 (2017).
- [22] P. Comaron, G. Dagvadorj, A. Zamora, I. Carusotto, N. P. Proukakis, and M. H. Szymańska, Dynamical critical exponents in driven-dissipative quantum systems, *Phys. Rev. Lett.* **121**, 095302 (2018).
- [23] M.-J. Hwang, P. Rabl, and M. B. Plenio, Dissipative phase transition in the open quantum rabi model, *Phys. Rev. A* **97**, 013825 (2018).
- [24] J. T. Young, A. V. Gorshkov, M. Foss-Feig, and M. F. Maghrebi, Nonequilibrium fixed points of coupled ising models, *Phys. Rev. X* **10**, 011039 (2020).
- [25] S. Pilgram, A. N. Jordan, E. V. Sukhorukov, and M. Büttiker, Stochastic path integral formulation of full counting statistics, *Phys. Rev. Lett.* **90**, 206801 (2003).
- [26] V. Elgart and A. Kamenev, Rare event statistics in reaction-diffusion systems, *Phys. Rev. E* **70**, 041106 (2004).
- [27] A. N. Jordan, E. V. Sukhorukov, and S. Pilgram, Fluctuation statistics in networks: A stochastic path integral approach, *Journal of Mathematical Physics* **45** (11), 4386 (2004).
- [28] A. N. Jordan and E. V. Sukhorukov, Transport statistics of bistable systems, *Phys. Rev. Lett.* **93**, 260604 (2004).
- [29] C. Padurariu, F. Hassler, and Y. V. Nazarov, Statistics of radiation at josephson parametric resonance, *Phys. Rev. B* **86**, 054514 (2012).
- [30] A. Chantasri and A. N. Jordan, Stochastic path-integral formalism for continuous quantum measurement, *Phys. Rev. A* **92**, 032125 (2015).
- [31] R. Vyas and S. Singh, Photon-counting statistics of the degenerate optical parametric oscillator, *Phys. Rev. A* **40**, 5147 (1989).
- [32] R. Vyas, Photon-counting statistics of the subthreshold nondegenerate parametric oscillator, *Phys. Rev. A* **46**, 395 (1992).
- [33] L. Arndt and F. Hassler, Statistics of radiation due to nondegenerate josephson parametric down-conversion, *Phys. Rev. B* **100**, 014505 (2019).
- [34] A. del Campo, Universal statistics of topological defects formed in a quantum phase transition, *Phys. Rev. Lett.* **121**, 200601 (2018).
- [35] F. J. Gómez-Ruiz, J. J. Mayo, and A. del Campo, Full counting statistics of topological defects after crossing a phase transition, *Phys. Rev. Lett.* **124**, 240602 (2020).
- [36] G. C. Duarte-Filho, F. A. G. Almeida, S. Rodríguez-Pérez, and A. M. S. Macêdo, Charge counting statistics and weak localization in a quantum chain, *Phys. Rev. B* **87**, 075404 (2013).
- [37] Y. Baek, Y. Kafri, and V. Lecomte, Finite-size and finite-time effects in large deviation functions near dynamical symmetry breaking transitions, *Journal of Statistical Mechanics: Theory and Experiment* **2019** (10), 103202 (2019).
- [38] G. E. Crooks, Entropy production fluctuation theorem and the nonequilibrium work relation for free energy dif-

- ferences, Phys. Rev. E **60**, 2721 (1999).
- [39] M. Esposito, U. Harbola, and S. Mukamel, Nonequilibrium fluctuations, fluctuation theorems, and counting statistics in quantum systems, Rev. Mod. Phys. **81**, 1665 (2009).
- [40] S. Schmidt and G. Blatter, Strong coupling theory for the jaynes-cummings-hubbard model, Phys. Rev. Lett. **103**, 086403 (2009).
- [41] I. Carusotto, D. Gerace, H. E. Tureci, S. De Liberato, C. Ciuti, and A. Imamoglu, Fermionized photons in an array of driven dissipative nonlinear cavities, Phys. Rev. Lett. **103**, 033601 (2009).
- [42] A. Schmid, On a quasiclassical langevin equation, Journal of Low Temperature Physics **49** (5), 609 (1982).
- [43] H. Kleinert and S. Shabanov, Quantum langevin equation from forward-backward path integral, Physics Letters A **200** (3), 224 (1995).
- [44] Note that at finite temperatures, we have  $\beta \mapsto \alpha(1+2n_B)$  with  $n_B = (e^{\hbar\Omega/k_B T} - 1)^{-1}$  and we obtain the classical limit with  $k_B T \gg \hbar\Omega$ .
- [45] Note that the dissipative part of the force can be included via the substitution  $a \mapsto a - 1$ .
- [46] Since the bifurcation is symmetric in  $b$ , we simplify the notation by focusing on the case  $b > 0$ .
- [47] B. Fiedler, S. Yanchuk, V. Flunkert, P. Hövel, H.-J. Wünsche, and E. Schöll, Delay stabilization of rotating waves near fold bifurcation and application to all-optical control of a semiconductor laser, Phys. Rev. E **77**, 066207 (2008).
- [48] We also want to neglect the broadening of the Josephson emission line by low-frequency phase noise. It can be neglected, if it is much smaller than the linewidth of the resonator  $\hbar\Gamma \gg \alpha k_B T$  [49, 50].
- [49] K. K. Likharev, *Dynamics of Josephson Junctions and Circuits* (Gordon and Breach Science Publishers, 1986).
- [50] L. Arndt, A. Roy, and F. Hassler, Dual shapiro steps of a phase-slip junction in the presence of a parasitic capacitance, Phys. Rev. B **98**, 014525 (2018).